How do Traffic Signs look like in Radar?

Klaudius Werber*, Michael Barjenbruch†, Jens Klappstein*, Jürgen Dickmann* and Christian Waldschmidt‡

*Daimler AG, Research Center Ulm, Team Active Sensors, Ulm, Germany
†Ulm University, Institute of Measurement, Control and Microtechnology, Ulm, Germany
‡Ulm University, Institute of Microwave Techniques, Ulm, Germany

***Abstract*—In this paper RCS measurements of traffic signs, a sign pole and a guide post for different viewing angles are presented. The signs show strongly angle dependent reflection characteristics and several sources of reflections. Furthermore, the effects of these characteristics relevant for a vehicle approaching a traffic sign are regarded.**

These considerations constitute a basis for using such traffic objects as landmarks for radar based vehicle self-localization.

I. Introduction

Future vehicles will offer more and more autonomous driving functions to reduce the driver's level of occupation necessary for driving. These functions will require information on the current vehicle pose (i.e. position and orientation) that is both accurate and constantly available. Both requirements are not met by current state of the art satellite based positioning systems (GPS, GLONASS, GALILEO). The position uncertainty of these systems is up to 10 m due to atmospheric disturbances or multi-path propagation [1]. Also, in tunnels or next to high buildings not enough satellites might be visible for the receiver and therefore no localization might be possible at all. Thus, new ways to reach higher pose accuracy and constant availability are necessary.

One possibility is to document landmarks (i.e. distinct areas with known global pose) along roads in a public database. Vehicles on a road can detect landmarks of this database in their neighborhood while driving. By finding the relative pose of the vehicle with respect to the landmarks in the neighborhood and by combining this relative position information with the global position information of the landmarks also stored in the database the vehicles can calculate their global pose.

This environment based approach has been applied with various sensor types, e.g. cameras or laser scanners [2], [3]. We want to adopt this approach for radar sensor data, because radar measurements are least affected by changing external conditions, for example between day and night or summer and winter. For this purpose, it is necessary to first investigate, how typical landmark candidates in a traffic environment are observed by a radar sensor. Therefore, in this paper we present results of radar measurements of typical traffic objects and derive a model for the radar amplitudes received by a vehicle approaching a traffic sign from these results.

II. Related Work

In [2] a camera has been used to detect features in the environment suitable for self-localization. Especially in cities and other man-made surroundings a camera usually finds a broad range of distinct features. But changes of the appearance of these features caused by different day-times, seasons or weather conditions often make recognition of these camera features a difficult task. In [3] a self-localization setup based on a laser scanner has been presented. Possible features for a laser scanner are rather similar to radar features. As an active sensor the laser scanner does not suffer from illumination changes between day and night. But as it operates in a frequency range close to visible light, the measurement performance also deteriorates with heavy weather conditions like rain or fog. In [4] a setup with a 77 GHz radar sensor has been used for vehicle self-localization based on radar reflector beacons as artificial landmarks. As we try to avoid the need of artificial landmarks, we emphasize on natural radar features that usually can be found along roads: on the one hand characteristic road shapes (e.g. junctions, not dealt with in this paper), on the other hand traffic signs and similar objects next to a road.

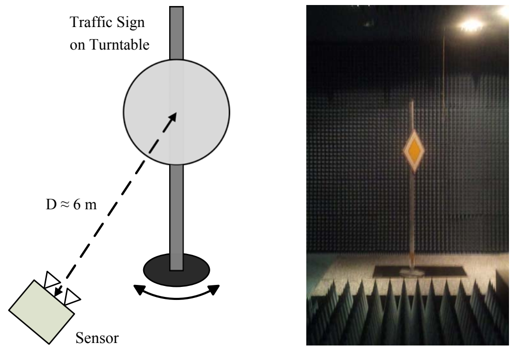

Fig. 1. Left: Measurement Setup
Right: Sign photographed from the sensor position

In [5] a setup rather similar to the one we present has been applied for characterization of various vehicles and a pedestrian. While these targets in traffic usually are moving, our scope is on objects that keep (at least temporarily) fixed positions and therefore can be used as (at least temporary) landmarks.

III. Radar Measurements

On the left side of Fig. 1 our setup for the RCS measurements of the objects introduced below is depicted. The sensor was aligned to point at the target that was fixed on a turntable in a distance of about 6 m to the sensor. The whole setup was

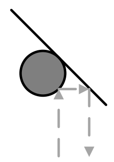

Fig. 2. Corner-like composition of pole and sign (top view)

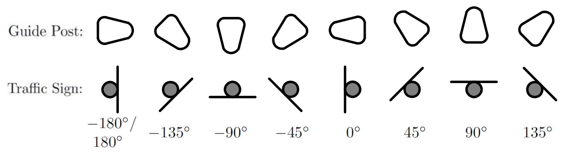

Fig. 3. Target orientation for different angles (top view)

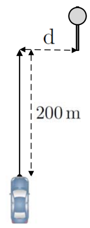

Fig. 4. Setup for sign approach simulation

contained in a radio-frequency unechoic chamber to damp any undesired reflections (cf. Fig. 1, right).

The following objects were measured in the given setup:

- **Two round traffic signs** of diameter 60 cm, one of reflection class 2 (RA2), the other one of reflection class 3 (RA3). As defined in [6] these classes describe the optical reflective strength of the synthetic cover material, RA2 being standard, RA3 indicating very strong reflections.
- **One square traffic sign** of side length 42 cm and reflection class RA2 (cf. Fig. 1, right)
- **One triangular traffic sign** of side length 90 cm and reflection class RA2
- **One guide post** made completely of polyethylene including some reflectors at the side

All signs are made of aluminum. For the measurements they were mounted on a galvanized steel pole of diameter 60.3 mm. Additional measurements were conducted with solely the pole and for RCS calibration with an aluminum sphere.

Measurements were recorded for every two degrees along one whole turn of the target. The mapping between an angle and the corresponding sign or guide post orientation is given in Fig. 3. There the shapes of the guide post and the traffic sign are depicted in top view for several orientations and it is assumed that the sensor is positioned below the figure facing upwards.

The results presented in the following section are based on measurements using a network analyzer. These measurements were conducted as S_{11} measurements with a vertically polarized horn antenna. For each angle of the target 11 frequency sweeps from 70 GHz to 80 GHz were done. The same measurements were repeated twice, once using an experimental automotive radar sensor operating at a center frequency of 77 GHz with a bandwidth of 600 MHz and once with a mass-production automotive long range radar sensor with a bandwidth of 150 MHz between 76 GHz and 77 GHz. The experimental radar operates with digital beam forming using chirp sequence modulation on 2 transmitting and 16 receiving antennas. The mass-production radar is a mechanically steered FMCW radar. Both measurement sets confirm the results of the network analyzer as presented in the next section.

IV. Results

The resulting RCS of the measured objects derived from the network analyzer measurements are shown in Fig. 8 for each individual angle. The standard deviation of each 11 measurements for the same target and angle is maximum −18 dB and on average −50 dB. Additionally, in Fig. 9 the range spectra of the same measurements are depicted showing the radial distance of the respective reflections. Points close to the center of the plots represent reflection sources close to the sensor. From both forms of representation the following deductions can be drawn:

Only the pole is rotation invariant. The guide post reflects strongly for all three flat sides oriented perpendicularly to the sensor (about −165°, −90°, −15°, 15°, 90°, −165°). If the reflecting plane is on the far side of the guide post thus occluded by the guide post itself, the amplitude only decreases slightly in comparison to the reflecting plane being in front. In general, both sides of the guide post do reflect, as can be seen from the two rings in the guide post plot of Fig. 9.

All traffic signs reflect very strongly if the sign plane is perpendicular to the sensor because of direct reflection. If the front of the round or triangular signs is facing the sensor not exactly perpendicularly, there is almost no back scattering. That shows that during the measurements the main lobe of the antenna was completely covered by the signs. Therefore, the pole behind the signs was not visible to the sensor. Some minor amplitude peaks due to edge diffraction can be observed in the sign plots of Fig. 9 along the two weak non-centered semicircles in the foreground. The damping effects are much weaker for the square sign. This sign has the smallest area and therefore seems to not cover the main lobe completely.

If the back of a sign is facing the sensor, there are two sources of strong reflections as indicated by the two strong semicircles in the background of the sign plots in Fig. 9. The inside circle has the same radial distance as the circle in the pole plot. This shows that these reflections are caused by the pole in front of the sign. The second further outside circle tends to the same radial distance as the sign plane for angles close to 90°. For angles closer to 0° and 180° the radial distance slightly decreases, while the amplitude values slightly increase. For angles about 0° and 180° this outside circle vanishes. We deduce that these reflections are caused by the corner-like composition of the pole and the plane (cf. Fig. 2).

There appear to be no remarkable differences in the characteristics of the two round signs with synthetic covers of different optical reflection classes. To verify this observation another experiment with the round sign of reflection class RA3 turned around (the covered side facing the pole) was conducted with a similar outcome as the presented results in the round sign plots of Fig. 8. This shows that the optical reflective cover material of traffic signs does not affect their radar characteristics.

To illustrate the effects of these rotation variant reflection characteristics of traffic signs several simulations of a vehicle approaching a traffic sign are presented below. For these simulations the following assumptions have been made:

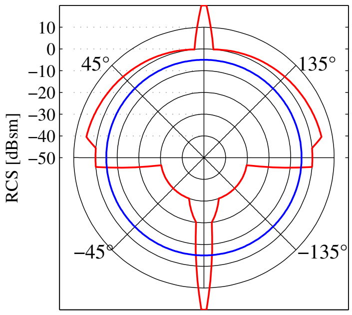

Fig. 5. Angular sign (red) and pole (blue) model

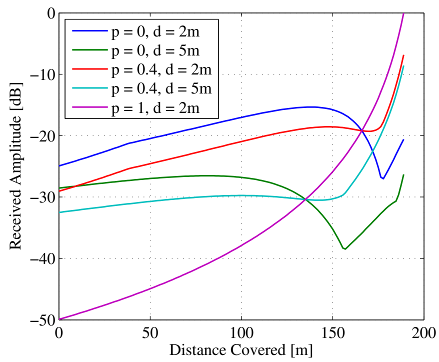

Fig. 6. Simulation results for different pole ratios p and cross-ranges d

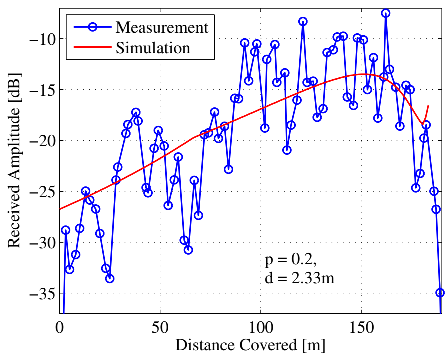

Fig. 7. Simulated and measured real sign approach

The sign is mounted on a pole 200 m in front of the vehicle radar sensor's starting position and slightly (d) misaligned in cross-range (cf. Fig. 4). Additionally, the sign is 2 m higher than the sensor. The vehicle then moves straight ahead causing the sight angle of the sign to drift away from nearly the right angle (i.e. $-90°$ in the plots of Fig. 8). As vehicle speed is assumed to only affect the number of observations of the traffic sign, speed is not regarded here.

For the angular reflection characteristics of a traffic sign and a pole the simplified models depicted in Fig. 5 are applied. These models are based on the results presented in Fig. 8. According to the radar equation for point targets (cf. [7]), the received signal amplitude is assumed to be proportional to the inverse of the square of the range between the sensor and the sign $(A \propto {}^1\!/_{r^2})$. As we do not regard linear sensor specific parameters (e.g. antenna gain), amplitude values in the following are relative magnitudes described in dB.

The sign and the pole are assumed to superpose linearly. Their ratio called pole ratio p here is a degree of freedom in the description of different signs (p = [0/1]: solely [sign/pole] effects).

Further effects like e.g. skewed signs, interference due to multi-path propagation by reflection on the road surface (cf. [8]), slight changes of the vehicle direction during approach or non-ideal sensor characteristics in range or angle are neglected here.

Fig. 6 shows the simulation results of various simulated drives approaching a sign. Especially in the plots with low pole ratio, one can see that the rotation variant reflection characteristics of the traffic signs can lead to counter-intuitive behavior of the received sign amplitudes while passing by a traffic sign on a road: The effect of increasing amplitude values due to decreasing distance to the sign while approaching can be overcompensated by the falling RCS values of the traffic sign for angles drifting away from the right angle.

While we do not claim to have exhaustively modeled all relevant effects that might occur when approaching a traffic sign (cf. two paragraphs above), by selecting the true cross-range and by fitting the best pole ratio it is possible to adjust the presented simulation to real measurements on public roads. That is done as an example in Fig. 7. The mean course of the measured data correlates to the simulated data. The differences between the simulation and the measurement on the one hand seem to be measurement noise and up to about 100 m sinus-shaped distortions that might stem from multi-path interference, cf. [8]. The strong rise and drop of the measured data close to 0 m and at about 180 m are due to the sign entering and leaving the sensor's field of view.

V. Conclusion

In this paper we have identified the main radar reflection sources of traffic signs and a plastic guide post. Additionally, we have shown that the radar reflection behavior of these typical road features is angle dependent.

That poses further constraints on the signal processing if a traffic sign is being used as a landmark. For detection and registration of a landmark sign not just the received radar amplitude for each radial distance is relevant, but also the respective angular configuration.

On the other hand, the rather strong reflections of traffic signs for distances far away from the sign observed in Fig. 6 make early detection of signs possible. Subsequently, evaluation for exact localization can be performed in close proximity of the sign exploiting the higher accuracy in cross-range. Our future work on this topic will be headed in this direction.

References

[1] I. Skog and P. Händel, "In-car positioning and navigation technologies - a survey." *IEEE Transactions on Intelligent Transportation Systems*, vol. 10, no. 1, pp. 4–21, 2009.

[2] O. Pink, "Bildbasierte Selbstlokalisierung von Straßenfahrzeugen," Ph.D. dissertation, Karlsruhe, 2011.

[3] A. Schindler, "Vehicle self-localization with high-precision digital maps," in *Intelligent Vehicles Symposium (IV), 2013 IEEE*, June 2013, pp. 141–146.

[4] S. Clark and H. F. Durrant-Whyte, "Autonomous land vehicle navigation using millimeter wave radar." in *ICRA*. IEEE Computer Society, 1998, pp. 3697–3702.

[5] K. Geary, J. Colburn, A. Bekaryan, S. Zeng, B. Litkouhi, and M. Murad, "Automotive radar target characterization from 22 to 29 ghz and 76 to 81 ghz," in *Radar Conference (RADAR), 2013 IEEE*, April 2013, pp. 1–6.

[6] *Retroreflektierende Materialien zur Verkehrssicherung Lichttechnische Mindestanforderungen an Reflexstoffe*, DIN 67520 Std., October 2013.

[7] M. Skolnik, *Radar Handbook, Third Edition*. McGraw-Hill Education, 2008.

[8] F. Diewald, J. Klappstein, F. Sarholz, J. Dickmann, and K. Dietmayer, "Radar-interference-based bridge identification for collision avoidance systems." in *Intelligent Vehicles Symposium*. IEEE, 2011, pp. 113–118.

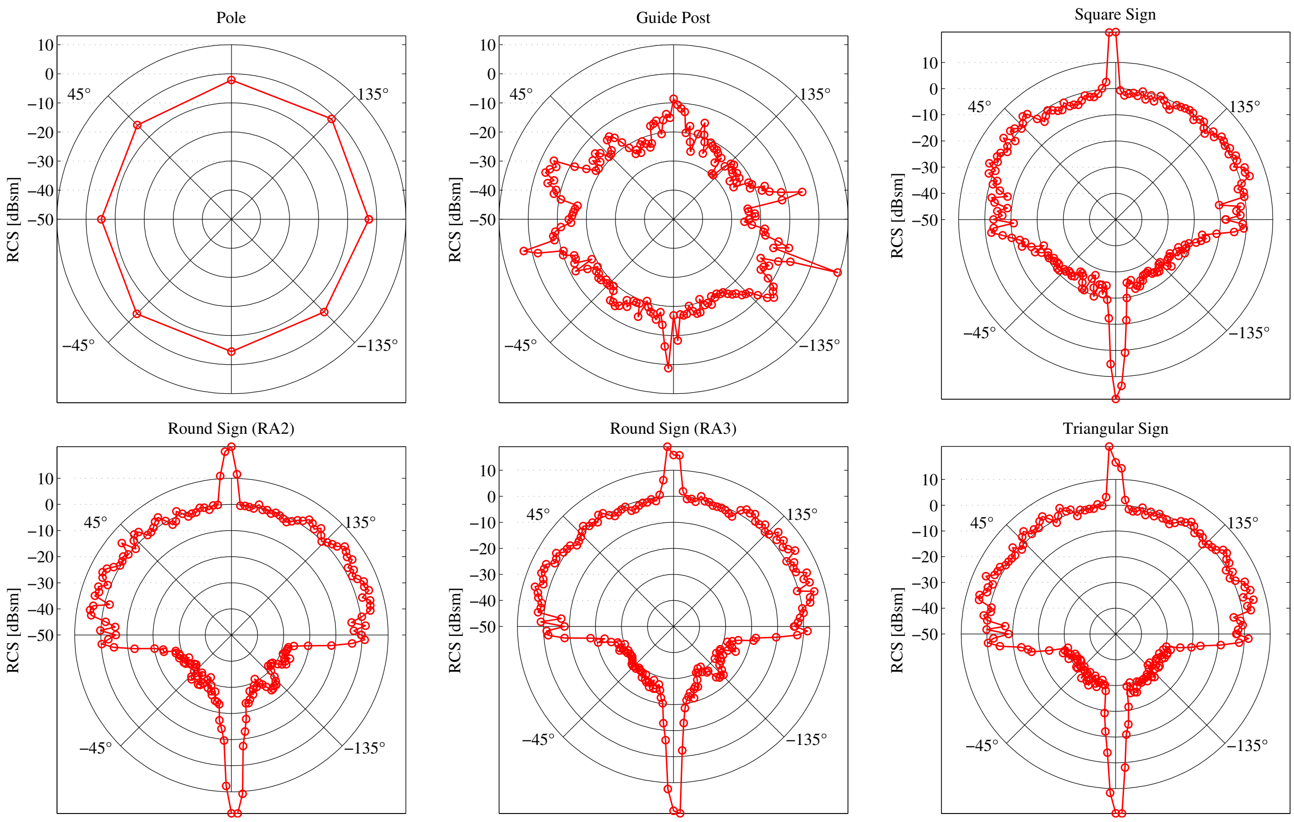

Fig. 8. Resulting angular diagrams of network analyzer measurements

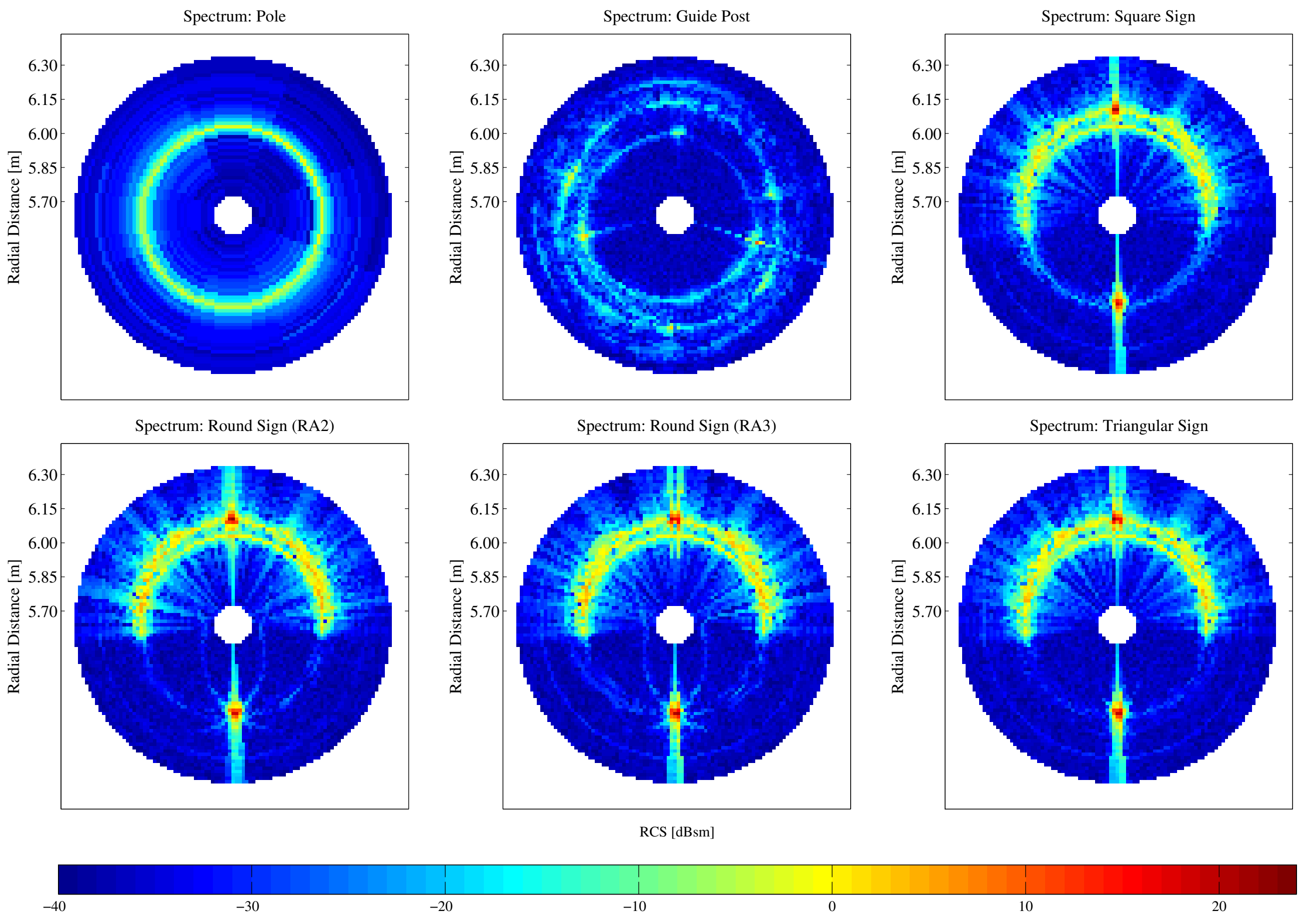

Fig. 9. Angular range spectra of network analyzer measurements